



“Preliminary” PhD Thesis

Biocompatible Thin Film Metallic Glasses (TFMGs)

PhD Candidate: Scott Gleason

Supervisor: Professor Michael Ferry

ABSTRACT

General abstract structure

Problem investigated

Procedures followed

Principle results obtained

Major conclusion reached

TABLE OF CONTENTS

Abstract.....	i
Table of Contents.....	ii
List of Figures	iv
1 Introduction	1
2 Proposal	1
2.1 Aims.....	1
2.1.1 TFMG Characterization	1
2.1.1.1 Substrates	1
2.1.1.2 Physical and Chemical Properties	1
2.1.1.3 Biocompatibility and Bioabsorption	1
2.1.1.4 Quality of Deposition	1
2.2 Methods.....	2
2.2.1 Magnetron Sputtering	2
2.2.1.1 Initial Sputtering Methods and Parameters.....	2
2.2.1.2 Target Preparation and Notes.....	2
2.2.1.3 Substrates Preparation and Notes.....	2
3 Literature Survey.....	3
3.1 Metallic Glasses (MGs).....	3
3.1.1 MGs Properties	3
3.1.2 Production.....	3
3.1.2.1 Solidification, Super Cooled Liquid (SCL), and Glass Transition (<i>T_g</i>)	4
3.1.2.2 Glass Forming Ability (GFA).....	5
3.2 Thin Films	7
3.2.1 Deposition	7
3.2.1.1 Pulsed Laser Deposition (PLD)	7
3.2.1.2 Sputtering Deposition	8
3.2.1.2.1 Direct Current (DC) Sputtering.....	8
3.2.1.2.2 Magnetron Sputtering	9
3.2.2 Thin Film Properties	10
3.2.3 Thin Film Adhesion.....	10
3.2.4 Ultrastable Metallic Glass (SMG)	10
3.2.4.1 SMG Production	10
3.2.4.1.1 Potential Production Issues	10
3.2.4.2 SMG Properties and Characteristics	11

3.2.4.2.1	Differential Scanning Calorimetry (DSC), Kinetic Stability and Enthalpy	11
3.2.4.2.2	The Theoretical Entropy Limit of Glasses and the Kauzmann Temperature T_k	12
3.2.4.2.3	Glass Fragility m	13
3.2.4.2.4	Indentation Modulus M	15
3.3	Biomedical.....	16
3.3.1	Bioreabsorption / Corrosion	16
3.3.2	Anti-biotic Scaffolds	16
4	References	17
5	Appendices.....	19
5.1	Glossary.....	19

LIST OF FIGURES

Figure 1: Schematic of specific enthalpy (h) and specific volume (V_{sp}) as a function of temperature for a material that exhibits both glass and crystalline solid states. Note 'glass 1' has a greater T_g and higher specific volume than 'glass 2.' This higher temperature stability is the result of 'glass 1' be cooled more quickly than 'glass 2.' Modified from [5].	5
Figure 2: Schematic TTT diagram where line (1) indicates the rapid cooling rate required to achieve the metallic glass state, and line (2) the processing window at elevated temperature above T_g which available to metallic glass. Reproduced from [7].	6
Figure 3: Schematic of a typical PLD setup showing the incoming laser beam inclined at an approximate 45° angle to the target, and the target and substrate parallel to each other. Adapted from [8].	7
Figure 4: Amorphous target XRD scan before (black curve) and after (red curve) PLD showing the shift from characteristic amorphous structure to crystalline. Reproduced from [11].	8
Figure 5: Schematic of a typical DC sputtering setup with an Ar working gas. The high-voltage field generates and propels Ar^+ ions toward the negative target of material "M." Dislodged "M" atoms are hurled in all directions with some being deposited on the positive substrate. Adapted from [12].	9
Figure 6: An integrated DSC trace for the molecular IMC glass system displaying the various values of T_f obtained when varying the deposition rate (the coloured line). Note all deposited glasses have a reduced T_f indicating a reduction in enthalpy compared to ordinary glass. Reproduced from [25].	12
Figure 7: Schematic of solidification/liquid glass temperature vs entropy in a typical glass forming system. The Kauzmann temperature (T_k) represents the glass transition temperature (T_g) of an ideal glass. The blue curve is the ideal path. Reproduced from [25].	13
Figure 8: Schematic of fragility for strong and weak glasses over the liquid range of viscosities. Note the 'ideal' strong liquid display a constant exponential slope over the full temperature range, while weaker liquids' slopes change. Reproduced from [27].	14
Figure 9: Schematic of the relationship between glass fragility (m) and the enhanced glass transition on glass transition ($\delta T_g/T_g$) for a selection of metallic, molecular, and polymer USGs. Reproduced from [1].	15

1 INTRODUCTION

Biocompatible films offer new possibilities in drug delivery and orthopaedic applications. Coating pharmaceutical scaffolds with tailored bioabsorbable films could allow for slow release of drug packages such as antibiotics, antimicrobials, and analgesics (painkillers). Films have also been shown to have significant effects on the properties of their substrates, which could allow for useful modification of orthopaedic devices like plates and fasteners. These application have the potential for great changes in wound healing and pain management.

2 PROPOSAL

2.1 AIMS

The aims of this thesis are to produce and investigate quality thin film metallic glasses (TFMGs) for biomedical applications. TFMGs of established bulk metallic glass (BMG) compositions, such as $\text{Mg}_{65}\text{Zn}_{30}\text{Ca}_5$ and $\text{Mg}_{65}\text{Cu}_{25}\text{Y}_{10}$, will be deposited on a number of different substrates. The properties and characteristics of the films as well as their effects on the different substrates will be investigated, and the characterised films compared with their BMG counterparts.

2.1.1 TFMG Characterization

The properties of the TFMGs will be investigated via characterising the films after application to different substrates, allowing standalone films as well as their effects on the substrates to be investigated.

2.1.1.1 Substrates

The substrates to be investigated are:

- No substrate (base TFMG only);
- Antimicrobial or Antibiotic-Infused polycaprolactone (PCL) Scaffolds; and
- BMGs of similar composition to the TFMGs.

2.1.1.2 Physical and Chemical Properties

The physical and chemical properties of the TFMGs will be characterized via a range of techniques; XRD, DSC, FIB-SEM, EPMA, ICP, etc.

2.1.1.3 Biocompatibility and Bioabsorption

The biocompatibility and bioabsorption of the TFMGs will be characterized via cytotoxicity testing, PDP scans, etc.

2.1.1.4 Quality of Deposition

The quality of the TFMG deposition will be ascertained via investigation of the surface finish, coating adhesion, bonding, etc.

2.2 METHODS

The TFMGs will be deposited onto the various substrates via physical vapour deposition (PVD) processes.

2.2.1 Magnetron Sputtering

Magnetron sputtering with an Ar working gas will be the preferred deposition technique, although pulse laser deposition (PLD) may be used as well (See section 3.2.1 Deposition).

2.2.1.1 Initial Sputtering Methods and Parameters

The initial sputtering parameters will be based on the work of Yu, et al. [1] on ultrastable $\text{Zr}_{65}\text{Cu}_{27.5}\text{Al}_{7.5}$ TFMGs and of Liu, et al. [2] on refining the deposition parameters for the $\text{Zr}_{55}\text{Cu}_{30}\text{Ni}_5\text{Al}_{10}$ TFMGs. These will be refined via appropriate step sizes as required to suit the examined biocompatible systems.

Parameters:

- Base chamber pressure: Better than 3×10^{-4} Pa (ideally better than 5×10^{-5} Pa);
- Deposition argon pressure: $5 \times 10^{-2} - 3.0$ Pa;
- Deposition power range: 30 – 50 W;
- Deposition Rate: To be determined via TEM, with an ideal rate of 1.4 nm s^{-1} ;
- Substrate deposition temperature: $0.7 - 0.8 T_g$;

2.2.1.2 Target Preparation and Notes

Targets will be crystalline alloys of $\text{Mg}_{65}\text{Zn}_{30}\text{Ca}_5$ and $\text{Mg}_{65}\text{Cu}_{25}\text{Y}_{10}$. The master alloys will be produced via induction furnace and formed via traditional casting techniques. Targets will be prepared for deposition via a pre-sputter to remove contamination and oxides from their surfaces.

2.2.1.3 Substrates Preparation and Notes

To produce the desired TFMGs the substrates will need to be at an elevated temperature of $0.7 - 0.8 T_g$. These temperatures will be achieved and controlled via a hot plate and thermocouple.

Furthermore, substrates will be prepared and procured as below:

- No substrate (base TFMG only);
 - TFMGs will be deposited onto NaCl wafer (or other water soluble) substrates;
 - NaCl wafers will be procured (not manufactured);
 - Films will later be separated from substrates via dissolving in water, or other manual removal methods;
- Antimicrobial or Antibiotic-Infused PCL Scaffolds;
 - PCL Scaffolds will be procured (not manufactured);
- BMGs of similar composition to the TFMGs;
 - BMG substrates will be produced from master alloys (see 2.2.1.2 Target Preparation and Notes) and amorphous casting techniques.

3 LITERATURE SURVEY

3.1 METALLIC GLASSES (MGs)

Metallic glasses (MGs) are alloys which exhibit an amorphous structure with no long range order. The materials generally display limited plastic deformation as the lack of a lattice structure greatly limits the potential for dislocation movement. However despite their limited slip systems, MGs are less brittle than organic glass owing to their non-directional metallic bonds [3].

Slow cooling

thus the materials absorb little energy and rebound elastically.

Multi-component alloys

Often near eutectic composition

Young Modulus 'E' about the same as crystalline alloy

High corrosion resistance owing to no grain boundaries.

Amorphous, no microstructure

3.1.1 MGs Properties

Low coefficient of friction

High hardness

High corrosion resistance

High wear resistance

High oxidation resistance

Slow heat conduction (limits casting)

UTS often greater than crystalline alloy

3.1.2 Production

The three rules of Inoue [4] are as:

- Multi-component systems (3 or more)

- Atomic size ratios above 12%

- Have negative heats of mixing (endothermic, ie reaction releases heat)

3.1.2.1 Solidification, Super Cooled Liquid (SCL), and Glass Transition (T_g)

Most liquid materials when cooled to their melting temperature (T_m) undergo a phase change into an ordered solid with a repeating crystalline structure. As this is a first-order thermodynamic phase change the entire process occurs solely at the T_m and is observed as an enthalpy (H) and volume (V) discontinuity. As the ordered structure is at a lower energy and generally more dense than the amorphous liquid both the H and V discontinuities are negative, with a notable exception being water where the V increases.

Despite the thermodynamic driving force liquids are generally cooled below their T_m before they begin to solidify because they require a stable nucleus to initiate the process. This solidification is described by Gibbs Free Energy Theory for homogeneous and heterogeneous nucleation. In brief, a stable nucleus initiates solidification by reaching a size where further growth requires less energy than melting providing the driving force for the phase change. Refer to "Gibbs Free Energy" for specific details which are not covered here within.

When the liquid is cooled below its T_m without solidifying it is termed a super cooled liquid (SCL). Amorphous solids, or glasses, are formed from SCL by cooling at rates sufficient to avoid the nucleation process entirely. As the SCL is cooled its viscosity (η) increases while its H and V decrease linearly with temperature at the same rate as the liquid state. As the η approaches about 10^{12} Pa*s the time scale for molecular rearrangement of the SCL becomes significantly longer than experimental observation and the SCL is for all practical purposes 'frozen' as a glass [5]. This transition occurs at the glass transition temperature (T_g) and is characterised by a decrease in rate of change of H and V with temperature. Note this is not a phase change, but a rather kinetic event, meaning the material is not technically thermodynamically or kinetically stable, even though it is stable for all intents and purposes [5]. Because of this the actual T_g of a glass depends on the cooling rate (i.e. is not a fixed property like T_m) with faster cooling rates generally resulting in higher T_g indicating the glass is suitable for use at higher service temperatures, see Figure 1.

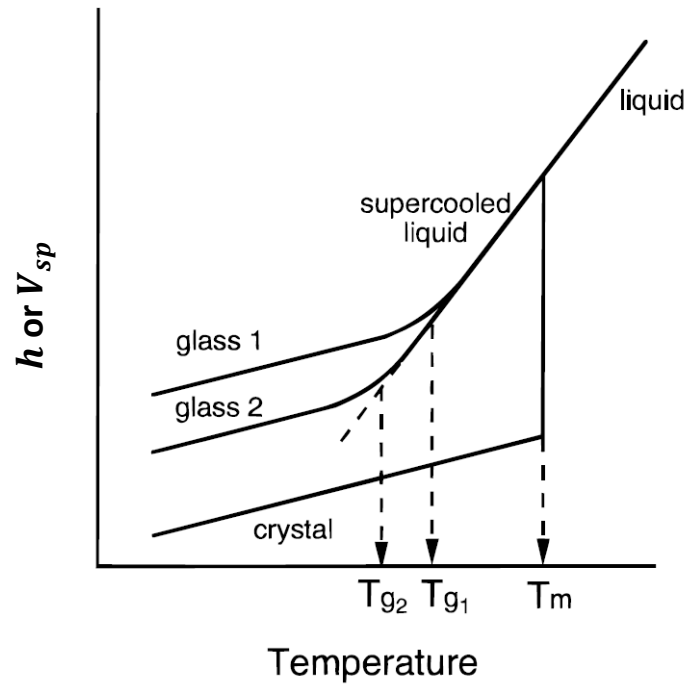


Figure 1: Schematic of specific enthalpy (h) and specific volume (V_{sp}) as a function of temperature for a material that exhibits both glass and crystalline solid states. Note 'glass 1' has a greater T_g and higher specific volume than 'glass 2.' This higher temperature stability is the result of 'glass 1' be cooled more quickly than 'glass 2.' Modified from [5].

3.1.2.2 Glass Forming Ability (GFA)

The ease at which a material is able to form a glass is termed its glass forming ability (GFA). Molecular glass' GFA is such that the material has been produced since agent times, and polymers' GFAs are often high enough they can form glass even with very slow cooling rates. This is in contrast to metals which have GFAs so low their amorphous glass state was only discovered as recently as 1960 by Klement, et al. [6].

GFA increases with T_g/T_m [4].

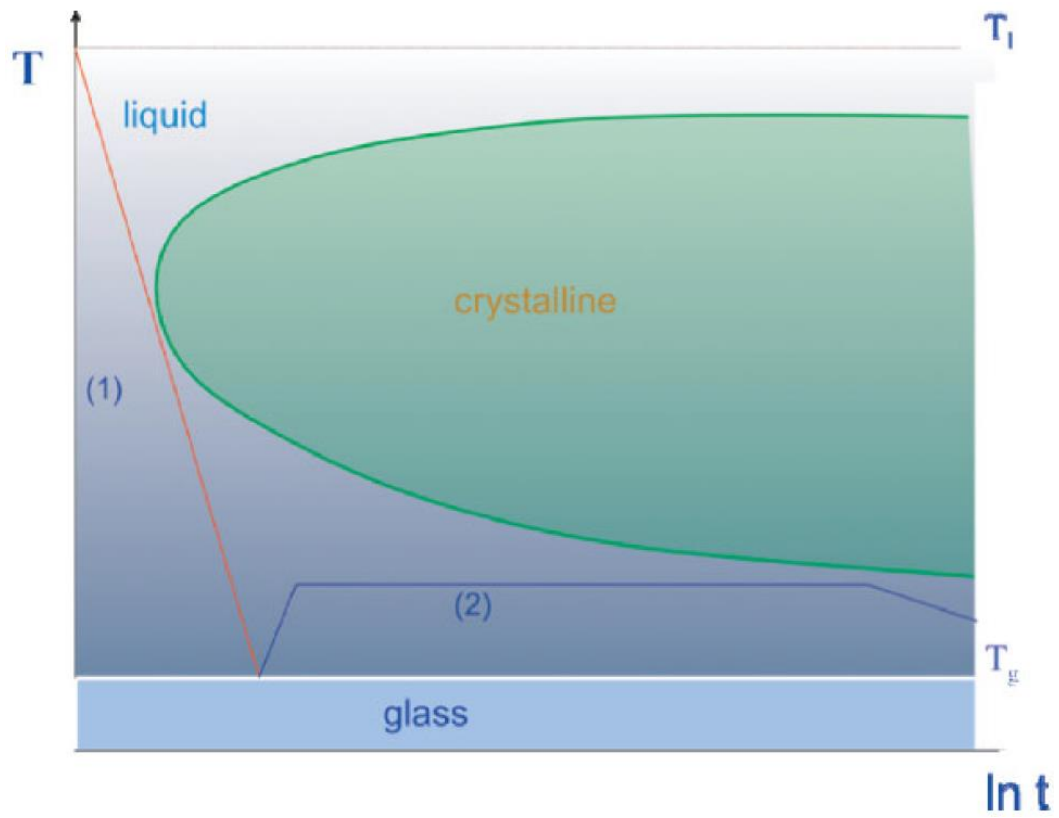


Figure 2: Schematic TTT diagram where line (1) indicates the rapid cooling rate required to achieve the metallic glass state, and line (2) the processing window at elevated temperature above T_g which available to metallic glass. Reproduced from [7].

3.2 THIN FILMS

3.2.1 Deposition

TFMG coatings are readily produced via vapour deposition (VD) processes such as the physical vapour deposition (PVD) processes of pulsed laser deposition (PLD) and sputtering. These processes produce the films by condensing vaporised material onto a solid substrate under low vacuum.

3.2.1.1 Pulsed Laser Deposition (PLD)

Pulsed laser deposition (PLD) produces films primarily via a thermal process under ultrahigh vacuum (UHV). The process requires a 'target' of the desired film material to be irradiated and locally vaporised by 45° inclined laser photon pulses. This results in a primarily perpendicular plasma plume of the target atoms directed toward the substrate, which on contact are deposited. Over the course of thousands of repetitions the build-up of atoms results in the film (Figure 3).

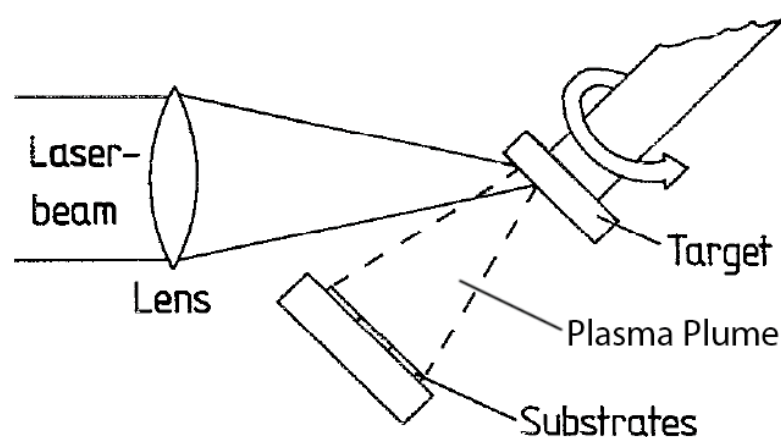


Figure 3: Schematic of a typical PLD setup showing the incoming laser beam inclined at an approximate 45° angle to the target, and the target and substrate parallel to each other. Adapted from [8].

The key advantage of PLD is it is able to deposit films of the same stoichiometric ratio as its targets [9, 10]. This is significant because it means deposited films have the same elemental composition as their target material. As the compositions of BMGs are generally carefully chosen this is practically useful as it streamlines achieving the desired TFMG compositions.

The work of Cao [11] has identified potential problems in PLD deposition of TFMGs with achieving quality surface finishes and recrystallization of amorphous targets. It appears the deposition times of the PLD allow for sufficient heat to be applied to amorphous targets to cause partial crystallisation (Figure 4), while still achieving amorphous TFMGs depositions onto the examined crystalline zirconium substrates. As PLD is by definition a thermal deposition process preventing this heat from entering the targets could be difficult. And it remains to be examined if this excess heat could affect the substrates; ie recrystallization of amorphous BMG, polycaprolactone (PCL) scaffolds strength, thermal breakdown of the scaffold payloads, etc. Naturally this heat is a moot point when examining standalone TFMGs as these specimens are separated from their substrate after deposition.

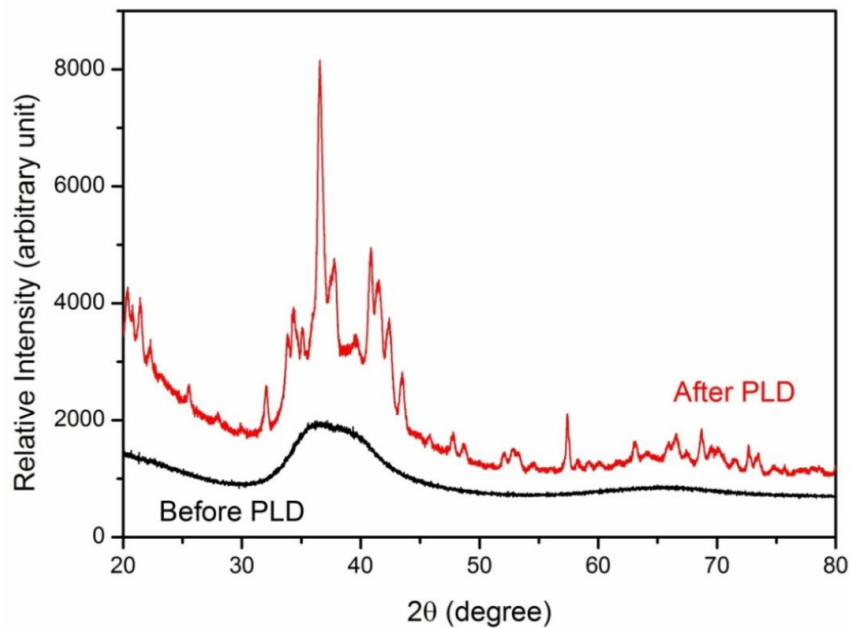


Figure 4: Amorphous target XRD scan before (black curve) and after (red curve) PLD showing the shift from characteristic amorphous structure to crystalline. Reproduced from [11].

PLD TFMG surface finish droplet defects have been observed by Krebs and Bremert [8] and later Cao [11]. It is suggested these defaults are intrinsic to the setup configuration and cannot be eliminated by refining the parameters. It is further proposed it may be possible to achieve higher quality surface finishes with setup modifications such as the addition of a mechanical velocity filter to remove slower, droplet depositing prone particles from the plasma plume. Another option is dual-beam ablation geometry which utilized two colliding laser ablation to redirect the coating to a substrate outside the direct path of both plumes preventing heavier droplet depositing prone particles from reaching the substrate. Notes both of these methodologies reduce the deposition rate and it remains to be seen if these changes are practical to implicate at UNSW.

3.2.1.2 Sputtering Deposition

Sputtering deposition is similar to PLD in that it coats a substrate with material transferred from a target, the essential difference being that it utilises the momentum of colliding ions, instead of lasers, to accomplish the transfer.

3.2.1.2.1 Direct Current (DC) Sputtering

Direct Current (DC) sputtering applies a high-voltage to create a circuit between the target and substrate, forming a negative (cathode) and positive (anode) electrode respectively. The high-voltage field generated within the chamber ionises the low pressure inert working gas, generally Argon, causing the now positive ions to be attracted to the negative target. The charged ions collide with the target and dislodge atoms as a plasma from its surface, which are expelled in all directions. A portion of these free atoms come in contact with the substrate surface and are deposited as the coating (Figure 5).

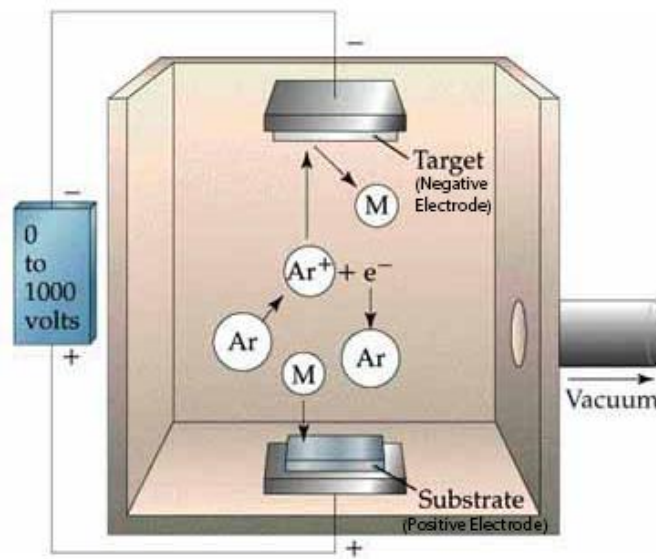


Figure 5: Schematic of a typical DC sputtering setup with an Ar working gas. The high-voltage field generates and propels Ar^+ ions toward the negative target of material "M." Dislodged "M" atoms are hurled in all directions with some being deposited on the positive substrate. Adapted from [12].

The key advantage of DC sputtering when working with amorphous materials is it able to accommodate low working temperatures as the mechanical mechanism avoids adding unnecessary heat to targets and substrates. Additionally, while Ar is a convenient working gas, greater deposition efficiency can be achieved when coating with lighter or heavier elements by working with lighter or heavier inert gases, respectively. These characteristics help make it possible to deposit most BMGs via DC sputtering.

3.2.1.2.2 Magnetron Sputtering

Magnetron sputtering is a variant of DC sputtering which improves ionisation efficiency by applying a magnetic field to trap the charged Ar^+ ions near the target surface. This variant has proven popular in recent studies and all further mention of sputtering shall be magnetron sputtering, unless otherwise noted.

While the momentum exchange mechanism of sputtering allows for the use of amorphous targets when depositing TFMG (ie excess heat is not added to the system) it has been found the use of crystalline targets results in no appreciable difference in the quality, composition, and structure of the substrate coating [2]. Instead, as shown by Liu, et al. [2] work on the $\text{Zr}_{55}\text{Cu}_{30}\text{Ni}_5\text{Al}_{10}$ system, the coating quality and production of TFMG is primarily controlled by the Ar pressure and sputtering power parameters. This has implication for practical application production runs as crystalline targets are easier and cheaper to produce than amorphous ones.

When depositing TFMGs it has been observed the deposition rate is proportional to the sputtering power, and that higher rates result in smoother film surfaces [2, 11]. Additionally, Liu, et al. [2] have found a dynamic smoothing effect occurs making it possible to produce atomically flat TFMGs with low Ar pressure and high sputtering power.

One of the core challenges with single target magnetron sputtering is it can be difficult to achieve the same composition as the target alloy when depositing multi-component TFMGs [2, 11, 13]. This can occur because of the different sputtering yield of composition target elements when subjected to ion bombardment. It is possible to remedy the situation through the use of multiple pure element targets, called combination deposition [14-16], but as shown by Liu, et al. [2] this method may not be

necessary. Liu, et al. [2] found it possible to deposit TFMGs with the same composition as their $\text{Zr}_{55}\text{Cu}_{30}\text{Ni}_{15}\text{Al}_{10}$ target by refining the Ar pressure and sputtering power parameters. As this solution requires only a single target and no modifications to the sputtering set up it seems reasonable to examine it first with Mg based systems.

Giving sputtering a number of advantages over PLD; non-thermal process, lower vacuum pressure, faster deposition rates, and smoother films.

3.2.2 Thin Film Properties

Thin films have been shown to increase a BMGs bending ductility [17].

3.2.3 Thin Film Adhesion

The adhesion of films is readily tested via scat methods [18-21].

3.2.4 Ultrastable Metallic Glass (SMG)

Ultrastable glasses (USGs) are amorphous films in a low energy state produced via VD techniques and generally characterised by their high thermodynamic and kinetic stabilities, densities, elastic moduli, and always by an enhanced glass transition temperature (δT_g). The δT_g phenomenon is their defining characteristic as it suggest the high kinetic stability because of the higher temperatures required to dislodge their atoms from the glassy configuration [22, 23]. This naturally extends to give USGs higher service temperatures, and hence higher melting temperatures relative to their traditional non-stable counterparts.

3.2.4.1 SMG Production

To date the only developed USGs are of organic glasses, molecular and polymer, with very few attempts being made to produce ultrastable metallic glasses (SMGs) [1]. Part of the reason for this is it unclear if the more simple atomic structures of metallic alloys, relativity to molecular and polymer glasses, are suitable to form USGs [1]. Nevertheless the work of Yu, et al. [1] on $\text{Zr}_{65}\text{Cu}_{27.5}\text{Al}_{7.5}$ has helped to established initial understanding of what appears to be SMGs, though it remains to be seen if the established trends extend to other metallic systems.

Production of USGs is via VD techniques onto a substrate at an elevated temperature. The initial work on USGs has shown the more complicated the deposition material's atomic structure the higher the substrate temperature (T_{sub}) needs to be [1]. Thus while the ideal T_{sub} for a MG is $0.7 - 0.8 T_g$, it is $0.75 - 0.85 T_g$ for the more complicated molecular glasses [1, 22-25]. Yu, et al. [1] goes on to note while it appears more complicated atomic structures require higher temperatures to arrange into USG configurations no definite mechanism has been identified for why USGs have ideal ranges well below their T_g , as higher temperatures would allow for efficient rearrangement of atoms.

The molecular relaxation kinetics of glasses are the reason VD techniques are required to produce the unique properties of USGs. This is easily demonstrated with organic glass where a reduction in cooling rate by a factor of 10 typically only decreases the T_g by about 3 kelvin [5, 23]. The results of the VD techniques cannot even be replicated with extensive artificial aging or annealing times below the T_g . For example Swallen, et al. [22] found with organic glass the ultrastable effects could not be replicated even when annealed below their T_g for 6 months, and when working with Kearns, et al. [25] went on to show the theoretical annealing time required would be at least 1000 years.

3.2.4.1.1 Potential Production Issues

Investigation has found there may be issues with the T_{sub} and PVD deposition rates when producing SMGs. For example, while it has been demonstrated an elevated T_{sub} is an inherent requirement to

produce USGs (see 3.2.4.1 SMG Production), Qin, et al. [15] found when working with the binary amorphous $\text{Zr}_{65}\text{Cu}_{35}$ system raising substrates to just room temperature could cause crystallization of the films. This appears concerning as the alloy constituents of this system are in comparable amounts with the Yu, et al. [1] $\text{Zr}_{65}\text{Cu}_{27.5}\text{Al}_{7.5}$ system. However this supports the theory that simple atomic structures metallic alloys may not be suitable to form SMGs, and it may be only more atomically complicated MGs, such as ternary systems, are suitable to form SMGs [1]. As this research will be working ternary Mg systems, it is believed they may be sufficiently atomically complicated to form SMGs.

It is known from Liu, et al. [2] and Cao [11] that higher deposition rates result in smoother TFMGs, though Kearns, et al. [25] work with molecular USGs have found lower deposition rates produce more kinetically stable, lower enthalpy glasses. Interestingly when Yu, et al. [1] produced SMGs they possess both high kinetic stability and high enthalpy (see 3.2.4.2 SMG Properties and Characteristics). As Yu, et al. [1] did not examine deposition rates this means it may be possible to produce lower enthalpy SMGs with lower deposition rates, although the films may become more rough. It is simply not known if the established deposition rates of TFMGs translate to SMGs.

3.2.4.2 SMG Properties and Characteristics

The defining characteristic of USG is an δT_g and accordingly high kinetic stability. They generally also are at a low-thermodynamic-energy state exhibited as a low enthalpy, have a high density, and possess a high elastic modulus.

3.2.4.2.1 Differential Scanning Calorimetry (DSC), Kinetic Stability and Enthalpy

Differential scanning calorimetry (DSC) is an analytical technique that measures the heat flow of an unknown sample. This is done by raising its temperature linearly at the same rate as a reference sample with a known heat capacity. This allows phase changes to be detected in the unknown sample as more or less heat will need to be applied to it to maintain both samples at the same temperature. This can be used to detect melting, crystallising, and more suitable changes like glass transition in a sample.

With amorphous materials the output displays an exothermic 'step in the baseline' as the sample reaches its T_g because it undergoes a change in its heat capacity. Upon further heating many amorphous materials spontaneously rearrange themselves in an ordered crystalline structure. This Crystallisation temperature (T_c) is recorded as an exothermic peak. With further heating the melting temperature (T_m) is reached and recorded as an endothermic peak, absorbing energy.

Using DSC the kinetic stability of glass can be measured by shifts in the onset temperature (T_{onset}), which appear as the first 'step in the baseline' in the DSC specific heat capacity (C_p) trace; identifying the start of the T_g region. Shifts in the T_{onset} to higher temperatures identify an increase in heat capacity as the atoms need to absorb more energy to become mobile; indicating the high kinetic stability with a higher T_g [25]. The value of the T_g is generally taken as the maxima of the derivative of trace with respect to temperature.

A specific enthalpy (h) curve from the DSC trace can be obtained by integrating the original C_p trace, with respect to temperature. Using this curve the fictive temperature (T_f) can be used to establish the enthalpy of the film by measuring where the film's enthalpy line intersects the extrapolated SCL enthalpy line of the bulk material (see Figure 6) [25]. A non-stable glass' enthalpy appears at $T_f = T_g$ on the trace, whereas a stable glass' is expected to have a lower T_f and lower enthalpy at $T_f < T_g$.

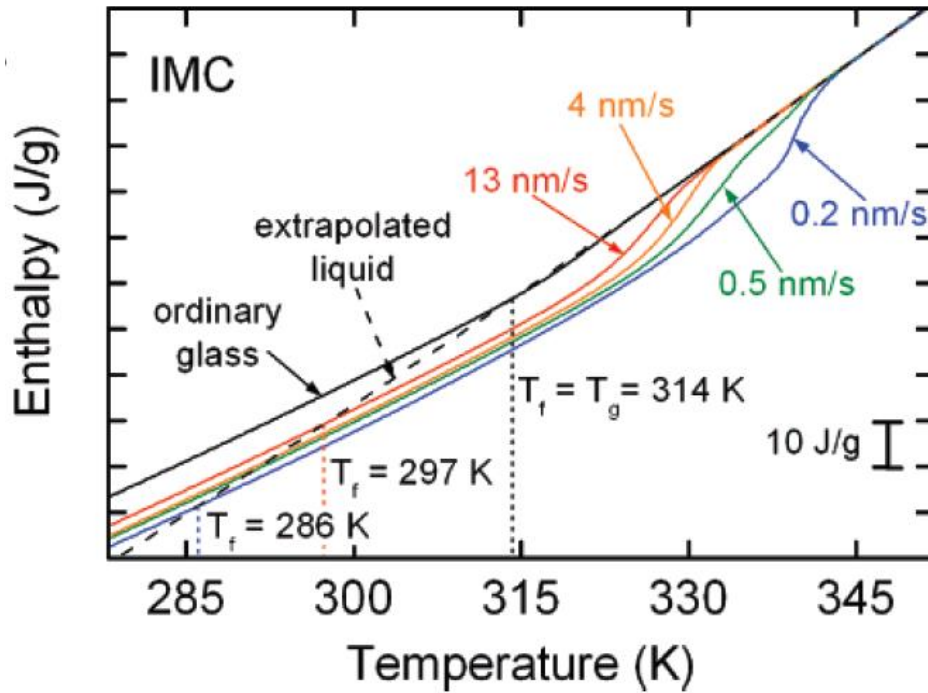


Figure 6: An integrated DSC trace for the molecular IMC glass system displaying the various values of T_f obtained when varying the deposition rate (the coloured line). Note all deposited glasses have a reduced T_f indicating a reduction in enthalpy compared to ordinary glass. Reproduced from [25].

However the work Yu, et al. [1] and Guo, et al. [26] on SMGs and polymer USGs respectively has shown an δT_g with its high kinetic stability can be coupled with high enthalpy. When this happens the enthalpy traces of USGs are greater than non-stable glass and intersect higher on the SCL line with a $T_f > T_g$. This contradiction with Kearns, et al. [25] demonstrates that T_{onset} and T_f are not coupled together and act independently in USG systems.

3.2.4.2.2 The Theoretical Entropy Limit of Glasses and the Kauzmann Temperature T_k

Normally a glass is formed when its SCL solidifies on reaching its T_g . However if the SCL can be lower to the entropy of its crystalline state it will achieve the theoretical lowest thermodynamic-energy state possible and its 'ideal' T_g , known as the Kauzmann temperature (T_k), see Figure 7 [22, 25]. This makes T_k a useful limit to evaluate the effectiveness of the improvements in thermodynamic stability of USGs.

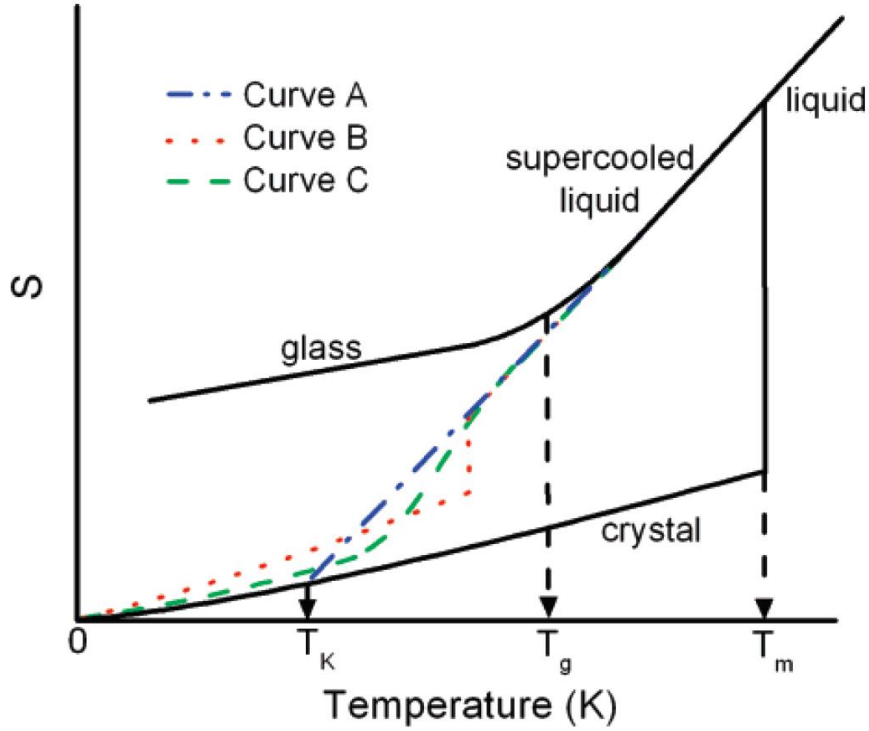


Figure 7: Schematic of solidification/liquid glass temperature vs entropy in a typical glass forming system. The Kauzmann temperature (T_K) represents the glass transition temperature (T_g) of an ideal glass. The blue curve is the ideal path. Reproduced from [25].

Using Swallen, et al. [22] and Kearns, et al. [25] equation for proportion along the energy landscape (θ_k) following 'Curve A,' the reduction in the glass' entropy compared to its non-stable variant can be calculated.

$$\theta_k = \frac{T_g - T_f}{T_g - T_K} \quad (3.1)$$

From equation (3.1) it can be seen a non-stable glass with $T_f = T_g$ will result in $\theta_k = 0$, signifying the glass has not moved down the energy landscape, while an ideal glass with $T_f = T_K$ will result in $\theta_k = 1$, signifying the glass has reached the bottom of the energy landscape [22, 25]. Therefore for real USGs with reduced entropy the θ_k will fall between 0 and 1, while the SMGs of Yu, et al. [1] which were found to have increased entropy would yield a θ_k of less than 0, indicating they have moving up the energy landscape. For example, a $\theta_k = -0.25$ would indicate the USG's entropy is 125% greater than the 'ideal' glass with a $T_g = T_K$.

3.2.4.2.3 Glass Fragility m

The fragility (m) of a glass is a measure of its deviation from ideal Arrhenius behaviour, defined by a function of variation in the glass' viscosity (η) with respect to temperature normalized by T_g .

$$m \equiv \left. \frac{\partial \log_{10}(\eta)}{\partial \left(\frac{T_g}{T}\right)} \right|_{T=T_g} \quad (3.2)$$

The more a glass varies from this ideal Arrhenius behaviour the more ‘fragile’ it is, and higher its m value. Highly fragile glasses vary greatly from the ideal Arrhenius behaviour and are termed ‘weak;’ generally experience significant deviations in heat capacity with temperature [27]. In contrast low fragility, or ‘strong’ glasses, have little variation from Arrhenius behaviour and usually experience little change in heat capacity with temperature. Whether a glass is strong or weak typically depends on the atomic structure, with MGs generally characterised as ‘strong’, polymers as ‘weak,’ and molecular glasses somewhere between, see Figure 8.

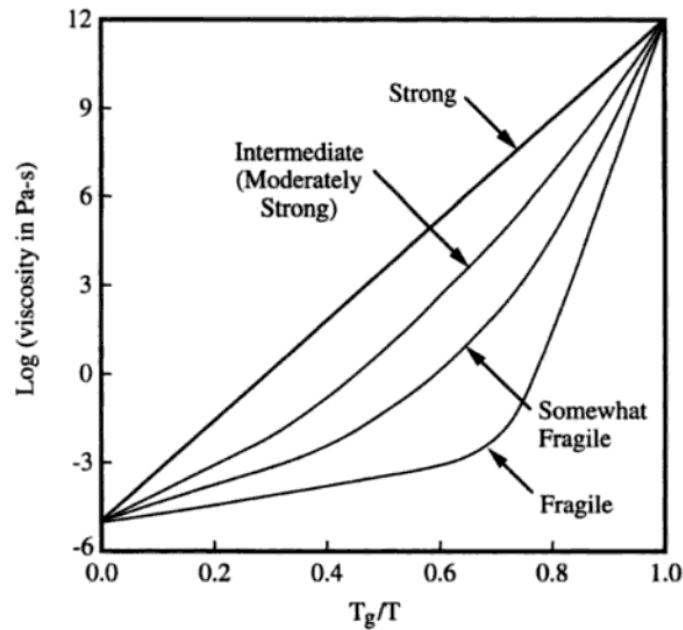


Figure 8: Schematic of fragility for strong and weak glasses over the liquid range of viscosities. Note the ‘ideal’ strong liquid display a constant exponential slope over the full temperature range, while weaker liquids’ slopes change. Reproduced from [27].

Yu, et al. [1] found m of metallic, molecular, and polymer USGs correlate with $\delta T_g/T_g$, which is surprising given the notable difference in their atomic structures, bonding, and deposition rates; see Figure 9. From these initial findings it appears greater improvements in δT_g in relation to the standard T_g correlates with more fragile glasses (i.e. a high m values supports a high δT_g). This suggests the δT_g improvements for SMGs may have a modest limit.

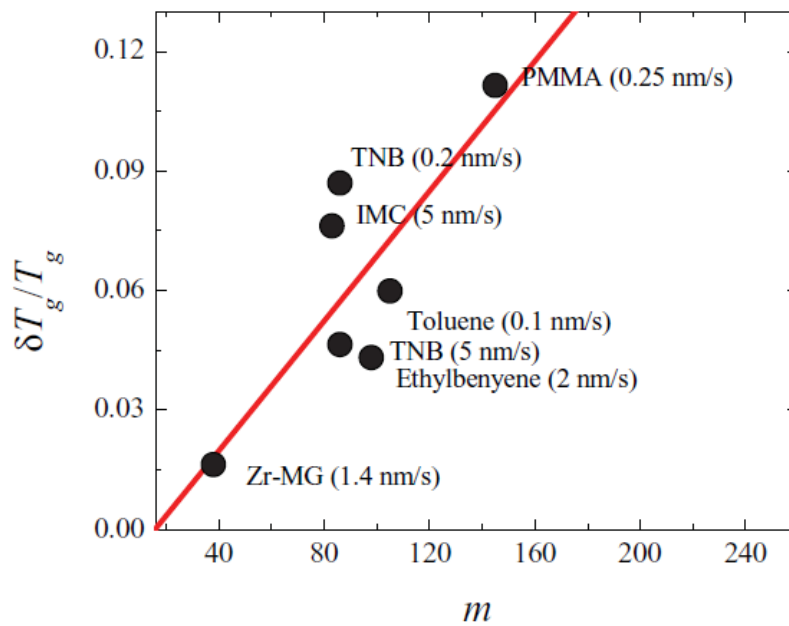


Figure 9: Schematic of the relationship between glass fridity (m) and the enhanced glass transition on glass transition ($\delta T_g/T_g$) for a selection of metallic, molecular, and polymer USGs. Reproduced from [1].

3.2.4.2.4 Indentation Modulus M

SMG has larger 'Indentation Modulus M ' than MG.

$$M \equiv \frac{E}{(1 - \nu^2)} \quad (3.3)$$

(around a 5 - 10% improvement from MG to SMG)

XRD cannot distinguish MG from SMGs.

(From molecular glasses (ie traditional glasses) would expect SMGs to show extra-low angle peaks)

May indicate a hidden polyamorphous or layer-like super-structures.

May indicate the corresponding states of packing are not drastically different.

It has been established that TFMGs displace different characteristics from BMGs. Coating of TFMGs directly onto BMGs can affect the BMGs characteristics. From "Bendable Metallic Glasses???"

3.3 BIOMEDICAL

Need to have section with the typical ranges of human bone hardness and E (most studies use these two parameters but do not include a human bone hardness for comparison).

3.3.1 Bioreabsorption / Corrosion

As Witte [28] has shown in his review magnesium was showing promise as a bioreabsorbable material in the early 1900s before the trend switch to bioinert materials like titanium.

Challenges with bioreabsorbable metals, need to;

- reduce the level of ion toxicity

- reduce the amount of hydrogen gas

- control the loss of mechanical strength over time.

High Zn content in MgZnCa decreases hydrogen evolution and promotes passive corrosion.

3.3.2 Anti-biotic Scaffolds

4 REFERENCES

- [1] H.-B. Yu, Y. Luo, and K. Samwer, "Ultrastable Metallic Glass," *Advanced Materials*, vol. 25, pp. 5904-5908, 2013.
- [2] Y. H. Liu, T. Fujita, A. Hirata, S. Li, H. W. Liu, W. Zhang, *et al.*, "Deposition of multicomponent metallic glass films by single-target magnetron sputtering," *Intermetallics*, vol. 21, pp. 105-114, 2// 2012.
- [3] A. L. Greer, Y. Q. Cheng, and E. Ma, "Shear bands in metallic glasses," *Materials Science and Engineering: R: Reports*, vol. 74, pp. 71-132, 4// 2013.
- [4] A. Inoue, "Stabilization of metallic supercooled liquid and bulk amorphous alloys," *Acta Materialia*, vol. 48, pp. 279-306, 1/1/ 2000.
- [5] M. Ediger, C. Angell, and S. R. Nagel, "Supercooled liquids and glasses," *The journal of physical chemistry*, vol. 100, pp. 13200-13212, 1996.
- [6] W. Klement, R. Willens, and P. Duwez, "Non-crystalline structure in solidified gold-silicon alloys," 1960.
- [7] J. Schroers, "Processing of Bulk Metallic Glass," *Advanced Materials*, vol. 22, pp. 1566-1597, 2010.
- [8] H. U. Krebs and O. Bremert, "Pulsed laser deposition of thin metallic alloys," *Applied Physics Letters*, vol. 62, pp. 2341-2343, 1993.
- [9] D. Dijkkamp, T. Venkatesan, X. Wu, S. Shaheen, N. Jisrawi, Y. Min-Lee, *et al.*, "Preparation of Y-Ba-Cu oxide superconductor thin films using pulsed laser evaporation from high T_c bulk material," *Applied Physics Letters*, vol. 51, pp. 619-621, 1987.
- [10] J. Heitz, X. Wang, P. Schwab, D. Bäuerle, and L. Schultz, "KrF laser-induced ablation and patterning of Y-Ba-Cu-O films," *Journal of Applied Physics*, vol. 68, pp. 2512-2514, 1990.
- [11] J. D. Cao, "Processing and properties of biocompatible metallic glasses," M. Ferry and K. Laws, Eds., ed: Thesis (Ph.D) - University of New South Wales - Australia, 2013.
- [12] T. E. Brown, T. L. Brown, H. E. H. LeMay, B. E. Bursten, C. Murphy, and P. Woodward, *Chemistry: The Central Science*: Pearson Education, 2014.
- [13] K. Kondoh, K. Kawabata, T. Serikawa, and H. Kimura, "Structural Characteristics and Crystallization of Metallic Glass Sputtered Films by Using Zr System Target," *Advances in Materials Science and Engineering*, vol. 2008, 2008.
- [14] Y. P. Deng, Y. F. Guan, J. D. Fowlkes, S. Q. Wen, F. X. Liu, G. M. Pharr, *et al.*, "A combinatorial thin film sputtering approach for synthesizing and characterizing ternary ZrCuAl metallic glasses," *Intermetallics*, vol. 15, pp. 1208-1216, 9// 2007.
- [15] J. Qin, X. Yong, Z. Xin-Yu, L. Gong, L. Li-Xin, X. Zhe, *et al.*, "Zr-Cu amorphous films prepared by magnetron co-sputtering deposition of pure Zr and Cu," *Chinese Physics Letters*, vol. 26, p. 086109, 2009.
- [16] M. Apreutesei, P. Steyer, L. Joly-Pottuz, A. Billard, J. Qiao, S. Cardinal, *et al.*, "Microstructural, thermal and mechanical behavior of co-sputtered binary Zr-Cu thin film metallic glasses," *Thin Solid Films*, vol. 561, pp. 53-59, 6/30/ 2014.
- [17] J. P. Chu, J. E. Greene, J. S. C. Jang, J. C. Huang, Y.-L. Shen, P. K. Liaw, *et al.*, "Bendable bulk metallic glass: Effects of a thin, adhesive, strong, and ductile coating," *Acta Materialia*, vol. 60, pp. 3226-3238, 4// 2012.
- [18] S. J. Bull and A. M. Jones, "Multilayer coatings for improved performance," *Surface and Coatings Technology*, vol. 78, pp. 173-184, 1// 1996.
- [19] P. J. Burnett and D. S. Rickerby, "The relationship between hardness and scratch adhesion," *Thin Solid Films*, vol. 154, pp. 403-416, 11/12/ 1987.
- [20] P. J. Burnett and D. S. Rickerby, "The scratch adhesion test: An elastic-plastic indentation analysis," *Thin Solid Films*, vol. 157, pp. 233-254, 2/29/ 1988.

- [21] C. T. Pan, T. T. Wu, C. F. Liu, C. Y. Su, W. J. Wang, and J. C. Huang, "Study of scratching Mg-based BMG using nanoindenter with Berkovich probe," *Materials Science and Engineering: A*, vol. 527, pp. 2342-2349, 4/15/ 2010.
- [22] S. F. Swallen, K. L. Kearns, M. K. Mapes, Y. S. Kim, R. J. McMahon, M. D. Ediger, *et al.*, "Organic glasses with exceptional thermodynamic and kinetic stability," *Science*, vol. 315, pp. 353-356, 2007.
- [23] K. Dawson, L. Zhu, L. A. Kopff, R. J. McMahon, L. Yu, and M. Ediger, "Highly stable vapor-deposited glasses of four tris-naphthylbenzene isomers," *The Journal of Physical Chemistry Letters*, vol. 2, pp. 2683-2687, 2011.
- [24] K. J. Dawson, L. Zhu, L. Yu, and M. Ediger, "Anisotropic structure and transformation kinetics of vapor-deposited indomethacin glasses," *The Journal of Physical Chemistry B*, vol. 115, pp. 455-463, 2010.
- [25] K. L. Kearns, S. F. Swallen, M. Ediger, T. Wu, Y. Sun, and L. Yu, "Hiking down the energy landscape: Progress toward the Kauzmann temperature via vapor deposition," *The Journal of Physical Chemistry B*, vol. 112, pp. 4934-4942, 2008.
- [26] Y. Guo, A. Morozov, D. Schneider, J. W. Chung, C. Zhang, M. Waldmann, *et al.*, "Ultrastable nanostructured polymer glasses," *Nature materials*, vol. 11, pp. 337-343, 2012.
- [27] J. E. Shelby, *Introduction to Glass Science and Technology*: Royal Society of Chemistry, 2005.
- [28] F. Witte, "The history of biodegradable magnesium implants: A review," *Acta Biomaterialia*, vol. 6, pp. 1680-1692, 5// 2010.

5 APPENDICES

5.1 GLOSSARY

BMG	–	Bulk Metallic Glass
C_p	–	Specific Heat Capacity (J/gK)
CVD	–	Chemical Vapour Deposition
DC	–	Direct Current (I)
DSC	–	Differential Scanning Calorimetry
GFA	–	Glass Forming Ability
H	–	Enthalpy (J)
h	–	Specific Enthalpy (J/g)
m	–	Fragility
MG	–	Metallic Glass
PCL	–	Polycaprolactone
PLD	–	Pulse Laser Deposition
PVD	–	Physical Vapour Deposition
SCL	–	Super Cooled Liquid
SMG	–	Ultrastable Metallic Glass
T_f	–	Fictive Temperature (K)
T_g	–	Glass Transition Temperature (K)
T_k	–	Kauzmann Temperature (K)
T_m	–	Melting Temperature (K)
T_{onset}	–	Onset Temperature (K)
T_{sub}	–	Substrate Temperature (K)
TFMG	–	Thin Film Metallic Glass
T_x	–	Crystallisation Temperature (K)
USG	–	Ultrastable Glass
V	–	Volume (m^3)
VD	–	Vapour Deposition
V_{sp}	–	Specific Volume (m^3/kg)

δT_g	–	Enhanced Glass Transition Temperature (K)
η	–	Viscosity ($Pa\ s$)
θ_k	–	Proportion along the Energy Landscape